Synthesis, Characterization and Study of Some of the Properties of $Zn_{1-x}Hg_xTe$ (x= 0 to 1) Thin Films

A. S. Rajbhoj[a], J.T. Deshmukh[a], A.B. Gaikwad[a], P.P. Hankare[b] and V. M. Bhuse[c*].

[a]Thin Films Laboratory, Department of Chemistry, Dr B.A.M. University, Aurangabad, India
[b]Department of Chemistry, Government Rajaram College, Kolhapur, India
[c]Department of Chemistry, Shivaji University, Kolhapur, India

_____

ABSTRACT

The present CdHgTe technology poses limitations on the efficiency of photovoltaic devices due to weakening of Hg-Te bonds by inclusion of Cd in CdHgTe. The major consequences are lattice mismatch, defects, low hardness and overall instability. Therefore, an equivalent, new material is being searched to resolve the issue. In view of this, we report, for the first time, a chemical route to grow a full range of ZnHgTe alloy system in thin film form. So far no literature is available on the synthesis of alloy system in thin film form using chemical bath method. The synthesis have been carried out using ammonia complexed mercury and zinc nitrates as a source of metal ions and sodium tellurosulphate, Na_2TeSO_3 (meta-stable), as a source of telluride ion at 323 K temperature. The films have been characterized by XRD, SEM, AAS, Optical absorption and Electrical measurement techniques. The XRD analysis of 'as deposited' thin films indicated cubic nature for all the films. The crystallinity, electrical conductivities were found to increase, while band gaps to decrease with addition of Hg progressively without any anomalies.

Keywords: Semiconductors, Chemical synthesis, X-ray diffraction, Scanning electron microscopy.
_____

INTRODUCTION

The thin film technology based on II–VI family of compound semiconductors, namely cadmium telluride (CdTe), zinc telluride (ZnTe) and mercury telluride (HgTe) has been the focus of great interest for applications in optoelectronics, including solar energy conversion [1–2]. Zinc mercury telluride (ZnHgTe, ZMT) is an alloy of mercury telluride (semimetal with n type conductivity) and zinc telluride (a direct gap semiconductor with 2.25 eV bandgap energy and p type conductivity). ZMT has better chemical, thermal, and mechanical stability than other ternaries of the same group.

440

_____

At present, the CdHgTe (CMT) is a variable band- gap system mostly used in the fabrication of photodetectors [3].   However, the existence of certain problems related to use of CMT, in particular, the instability of its lattice, surface, and interphase boundary, have initiated the development of alternative materials for application purpose [4]. A study based on theoretical considerations has shown that the weak HgTe bond is further destabilized by alloying it with CdTe, however, is stabilized by addition of ZnTe [5]. ZMT seems to occupy a prominent place over CMT due to following reasons; i) the ZnTe and HgTe systems, similar to CdTe and HgTe systems, can form a continuous series of solid solutions [6], ii) a host lattice of ZnTe is less destabilizing than that of CdTe [7], ii) ZMT exhibit better structural properties (such as micro-hardness and dislocation- formation energy) and fairly high mobilities of charge carriers [8, 9,10], iii) the composition and temperature dependence of the band gap in ZMT is more sensitive than that of CMT [11] and (iv) $Zn_{1-x}Hg_xTe$ films exhibit better coefficient of absorption.

So far, several bulk and epitaxial techniques like molecular beam epitaxy, chemical vapor deposition, liquid phase epitaxy, isothermal vapor phase epitaxy etc. are commonly employed techniques to evolve films [1, 5, 12-17]. These techniques are, however, costlier and require control over a number of parameters, moreover film grown by using these method suffers from nonstoichiometry and includes defects such as lattice mismatch, dislocations, elastic deformations, etc that affect severely the electrical characteristics. A high processing temperature, on the other hand, leads to chemisorption of oxygen and formation of unstable oxide layers on the surface, which may cause uncontrolled band bending and high interface recombination velocities in photovoltaic devices. Another method popularly used is electro-deposition, which involves gathering of 'atoms' randomly (not strictly in the given ratio), creating a sort of non-stoichiometry in deposits with impregnation of impurities. The electrodeposition may leads to agglomerated and fused grain structures..

In view of this, we propose a simple chemical deposition technique to evolve uniform, stoichiometric thin films. This method has been used successfully for deposition of alloys of CdHgSe [18], CdPbSe [19], CdZnSe [20] and ZnHgSe [21] in thin film form.

MATERIALS AND METHODS

All the chemicals used were Analytical Reagent grade (E. Merk). The solutions were prepared in doubly distilled water. Micro glass slides (Blue Star Co. Mumbai), cleaned successively by washing with chromic acid, water was used as substrate to deposit films.

2.1. Preparation of anionic precursor:
A metastable anionic precursor, sodium tellurosulphate, Na_2TeSO_3, was prepared by the method reported in our earlier paper [22]. The Na_2TeSO_3 is stable in hot condition, therefore, it was kept in an air tight container throughout at 318 K temperature.

2.2. Preparation of cationic precursor:
A cationic precursor solution was prepared by mixing appropriate volumes of (0.25 M) zinc nitrate and (0.25 M) mercuric nitrate solutions (corresponding to required composition) with complexing agent ammonia (25% v/v, 40 ml). For example, to prepare $Zn_{0.4}Hg_{0.6}Te$ films, a 4.0

_____

ml of (0.25 M) zinc nitrate and 6.0 ml of (0.25 M) mercuric nitrate solution was complexed with ammonia.

2.3. Preparation of thin film

To a cationic precursor solution, 1.0 ml of 1% hydrazine hydrate was added and the final volume made to 180 ml by adding distilled water. This beaker was transferred to a temperature controlled bath. A specially designed substrate holder, holding two cleaned glass slides was rotated vertically in the bath solution slowly (45 ± 5 rpm). The temperature of bath was then raised to 318 K slowly (within half hour). At this temperature, 10 ml of anionic precursor solution (preheated to 318 K) was added gradually and the stirring was continued with increase in temperature to 353 K within next 150 minutes. After about 3 hours, the glass slides coated with films were removed from bath, washed with hot distilled water and dried in dark desiccator under anhydrous $CaCl_2$.

2.4 Film characterization

X-ray traces of films were recorded using a Philips PW-1710 X-ray spectrophotometer with Cu Kα_1 line (1.54056Å) in 2θ range from 10-80$^\mathrm{o}$. The X-ray tube was operated at 20 kV, 20 mA with a scanning speed of 0.25 s per step. The optical absorption spectra were recorded in wavelength range of 350-2100 nm using a Hitachi-330 (Japan) double beam spectrophotometer at room temperature. The electrical resistance measurements were carried on Zintek-502BC Milliohmmeter in 300-500 K temperature range. A quick drying silver paste was applied for ohmic contact purpose. A 250MK-III Stereoscan (U.S.A) Scanning Electron Microscope (SEM) was used to observe surface morphology. Compositional analysis for elements was carried out by using Atomic absorption spectrophotometer.

RESULTS AND DISCUSSION

3.1. Film Growth

The process of film formation always requires a slow chemical precipitation of a given compound in the solution. The solubility product and the adhesion of the precipitate on the substrates are the important parameters on which film formation depends. The concentration of ions required to precipitate the compound must be greater than those given by solubility product. The solubility product of both, HgTe and ZnTe are low, therefore at low temperature all ions are in a stable, bound state so that no precipitation could be observed. A slow increase in temperature initiates the process of dissociation / decomposition of precursors giving bare ions so that the concentration of ions required to precipitate both is just exceed the solubility product (Ksp). For film formation, it is required that the nucleation should occur on the surface of the substrate. The nucleation (seeding) is the gathering of few ions in the initial stage. A local inhomogeneity or presence of some impurity may act as nucleation centre. The film formation requires the nucleation to take place on the substrate surface. If the nucleation occurs only in solution, we get precipitate and no film. Thus, adhesion of 'nucleolus' on substrate surface is essential in getting film. The precipitation reaction follow the usual steps; nucleation, growth and termination. The decomposition reactions in an ammoniacal media can be written as;

$$Na_2TeSO_3 + 2\,OH^- \Rightarrow \ Te^{2-} + Na_2SO_4 + \ H_2O \hspace{3cm} \ldots(1)$$

_____

$[Zn(NH_3)_4]^{2+} \Leftrightarrow Zn^{2+} + 4 NH_3$ (dissociation of Zn complex)   …(2)

$[Hg(NH_3)_4]^{2+} \Leftrightarrow Hg^{2+} + 4 NH_3$ (dissociation of Hg complex)   …(3)
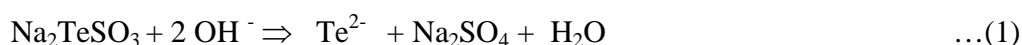
This reaction 1,2 and 3 gives Te^{-2}, Zn^{+2} and Hg^{+2} ions in the solution which combines to form film according to;

$(1-x) Zn^{2+} + x Hg^{2+} + Te^{2-} \Rightarrow Zn_{1-x}Hg_xTe$ …(4)
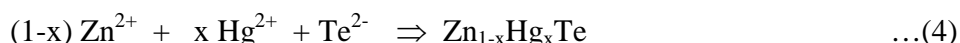
The overall reaction can be written as;

$1-x[Zn(NH_3)_4] + x[Hg(NH_3)_4] + Na_2TeSO_3 + 2OH^- \Rightarrow Zn_{1-x}Hg_xTe + 4 NH_3 + Na_2SO_4 + H_2O$
…(5)

During growth, a group of nuclei is converted to ZnHgTe by absorbing more and more Zn, Hg and Te ion, depending upon the availability of ions in the vicinity. A slow and uniform churning of the bath solution is quite essential to keep 'homogeneity' of ions in the vicinity and thus in film. An initial layer so formed further speed up the growth [23.22]. The chemical growth technique involves combination of 'cations' with 'anions' so that these oppositely charged ions, by virtue of electrostatic force of attraction (ionic bonding), can combine systematically and proportionately to result well ordered and stiochiometric materials / alloy. This 'ion by ion' combination has emerged as an important method to generate alloy (solid solution) even at low temperature (far lower than their melting point) as the oppositely charged 'ions' are getting combined rather than 'atoms' or 'molecules'[18-21].

The optimized conditions to get good quality films are; reactant concentration- 0.25 M, pH of the reaction Mixture: 10.5, precursor mixing temperature- 318 K, Final temperature- 353 K, Stirring rate- 45±2 rpm, deposition time -180 min. The color of CMT film was found to be grey with yellowish glare while that of ZnTe, it was faint yellow.

3.2 Structural, Morphological and Compositional Investigations
The XRD pattern of ZnTe, HgTe and few representatives ZMT are shown in Fig. 1. The pattern of as deposited ZnTe and HgTe showed a good match to those of standard cubic ZnTe (JCPDS card No 80-0022) and HgTe pattern (JCPDS card No 77-2014). While all other mixed composition films ($Zn_{1-x}Hg_xTe$) showed the line positions falling intermediate to those of the corresponding planes of the cubic ZnTe and HgTe. The peaks of ZMT have been identified as the reflections originating from 111, 200 & 220 Miller planes. A systematic shift of corresponding peak to lower 2θ positions with inclusion of mercury has been observed. The patterns showed no peaks belonging to hexagonal or individual phases. The cell constants of all the film samples have been computed using relation;

$$a = d(h^2 + k^2 + l^2)^{\frac{1}{2}}$$ …(6)

where h.k.l are Miller planes and d is inter planar distance. The values calculated are included in table 1. In general, the cell size was found to increase linearly with increase in concentration of

_____

mercury in ZnTe. The values of cell constants for each of the peak observed in the XRD pattern were also calculated and found to be almost similar indicating that the film deposited is homogeneous without any residual strain.

The cell size was found to vary linearly with the compositions following the Vegard's law. This kind of behavior have been reported for ZMT films by Sher et al [5], Thero et al [14]. The crystallinity was observed to be low for ZnTe film, while it increases with the composition parameter(x) indicating that the crystallinity increases with incorporation of mercury. The grains size was determined from strongest peak using the following Scherrer's equation and is included in table 1.

$$(t = 0.9 \lambda / bCos\theta) \qquad \qquad \ldots(7)$$

The grains size increase with increase in mercury content with the values falling between 250 to 350 Å. The increase in grain size can be correlated to increase in cell size due to addition of bigger Hg ion in the ZnTe lattice.
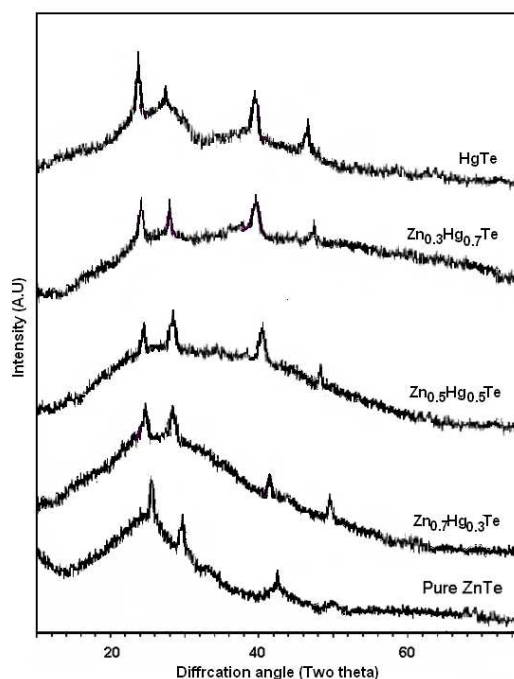
Figure 1: X ray diffraction pattern of CMT film recorded between two theta range of 10-80^{0} (X= 0.0,0.3, 0.5, 0.7 and 1.0)

The SEM photograph of ZnTe, HgTe and few representative ZnHgTe films (x=0.0, 0.1, 0.3, 0.5, 0.8 and 1.0) are shown in Figure 2. The film surface morphology was homogenous with grains well covered on the glass substrate, without any cracks or pinholes. The ZnTe showed somewhat amorphous behavior. The compactness, texture uniformity, grain size were enhanced with addition of mercury in ZnTe. The agglomeration and fusion of smaller crystallites, as usually observed in deposits obtained by electrodeposition are not observed in these films.

444

_____

Atomic absorption spectroscopy was used to determine the quantity of zinc and mercury content in the film samples as well as bath. A known weight of the film material was dissolved in the minimum quantity of concentrated nitric acid and used, after proper dilutions. The tellurium content was measured gravimetrically [24]. The concentration of zinc, mercury and tellurium present in the films were found to be proportional to those taken in bath within 3 to 5% error limit, indicating better stoichiometry of the films.
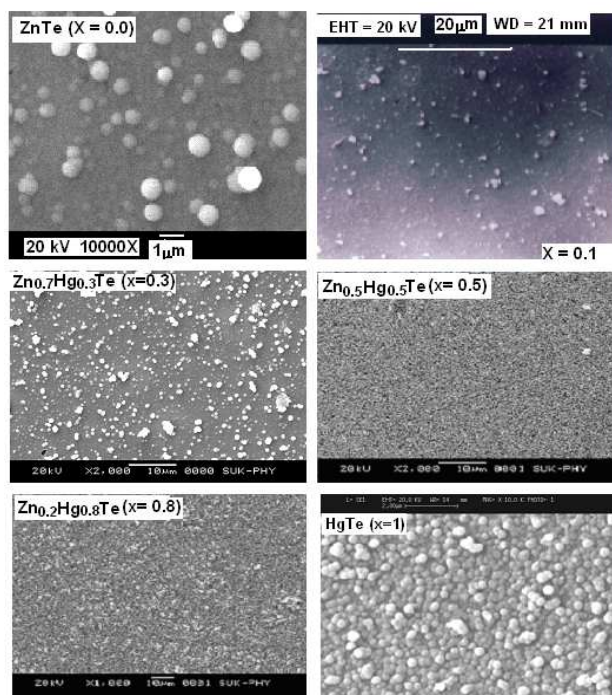
Figure 2: Scanning electron micrograph of ZMT (X =0.0, 0.1, 0.3, 0.5, 0.8 and 1.0)

3.3. Optical Properties

The measurements of absorption edge were carried out in the wavelength range from 350 to 2100 nm at room temperature. The absorption coefficients have been calculated from the absorption data. In general, the absorption coefficients were found to be high, of the order of 10^4 cm^{-1}. The absorption spectra of all the films showed presence of a single edge (steep rise in absorption) at room temperature corresponding to presence of a single type of band gap (figure not shown).   The important observation is that the absorption edge was shifted towards longer wavelength with increase in mercury content of the film.

The absorption spectra were analyzed on the basis of three dimensional model. According to it, the dependence of absorption coefficient in the vicinity of band edge is governed by;

$$\alpha h\nu = A (h\nu - Eg)^n \qquad\qquad \dots(8)$$

Where, A is absorption coefficient, hν is photon energy (eV), Eg is the band gap and n is a pure number that depends on the type of transition involved. For valid n (1/2 for direct transition, 3/2 for indirect transition), the equation (8) can be rearranged to y = mx + c form so that $(\alpha h\nu)^{1/n}$

_____

versus hν plot for hν > Eg can represent a line, the extrapolation of which to x axis could give magnitude of the optical band gap.
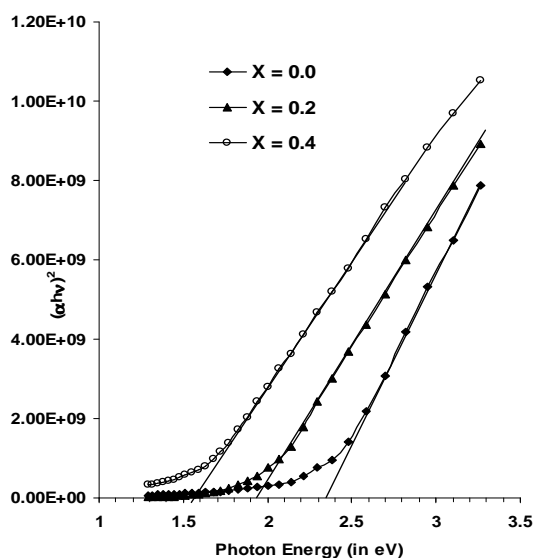
Fig 3a
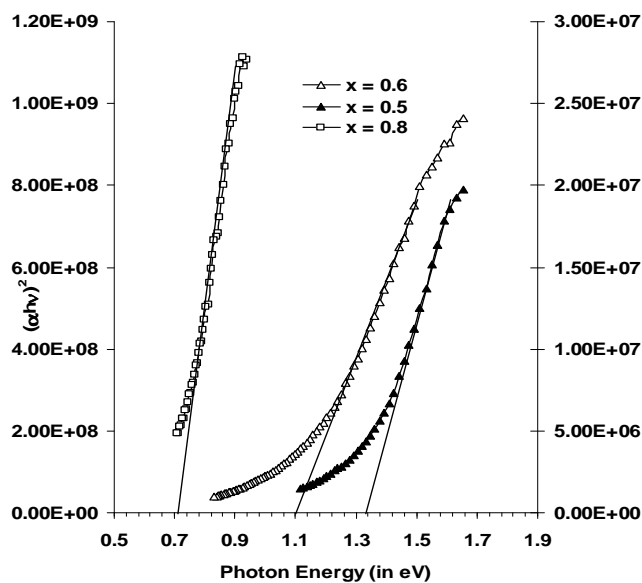
Figure 3b

Figure 3a &b : Band gap calculation [(αhν)^2 Vs hν plot] for films with x = 0.0, 0.2, 0. 4 (Fig. 3a), 0.5, 0.6 and 0.8(Fig. 3b)

Figure 3 a & b represents the (αhν)^2 versus hν plots for samples with x = 0.0, 0.2, 0.4 (Fig 3a), 0.5, 0.6, 0.8(Fig. 3b). For all the films, we observed the best fit at n = ½ indicating that the transitions involved are the direct allowed type. The values of band gaps computed from the plots are listed in Table 1. The magnitude of the band gaps for various compositions was decreased monotonically from 2.33 to 0.31 eV with increase in mole fraction of mercury(x). A gap of 2.33 eV was observed for ZnTe, matching roughly with the literature reported value (2.26

446

_____

eV) [22]. In case of HgTe, however, a large disparity exists in the magnitude of band gaps. The bulk HgTe was reported to have inverted type of gap with a negative gap of -0.3 eV [2], while in thin film form, the value reported is +0.3 eV [21]. As high as 2.14 eV band gap for polycrystalline HgTe film with crystallite size ~ 40-70Å have been reported in reference [25]. Petty and Juhasz [26] observed that the energy gaps of 1µm thick $Zn_xHg_{l-x}Te$ film with average of 1500Å grain size, prepared by co-evaporation technique passes through a 'zero-gap' at x = 0.1. In present investigation, we do not observe any negative value but instead, a positive gap of value 0.31 eV was observed. The positive band gap can be explained on the basis of following reasons; i) the grain size observed in our film is ~300Å, which is five times lower than that observed in reference [26]. The Bohrs radii of HgTe is large therefore, in thin film form, we expect a strong size quantization effect, ii) the electronic transitions involved are from heavy hole band to conduction band, therefore, the position of the absorption curve was largely influenced by the position of the Fermi level This give rise a well known shift, called Moss-Burstien shift.

3.5   Electrical and Thermo Electrical Properties

The dc electrical conduction mechanism of ZMT samples have been investigated as per Pertritz model [27] in 300-500K temperature range. The mechanism follows relation;

$$\sigma = \sigma_0 \exp(-\Delta E/kT) \qquad \qquad …(9)$$

Where σ is the conductivity, σ_0 is the constant, ΔE is the energy of activation, k is Boltzmann constant and T is the absolute temperature. The activation energy of conduction has been obtained from the slope of log σ vs. 1000/T plot.
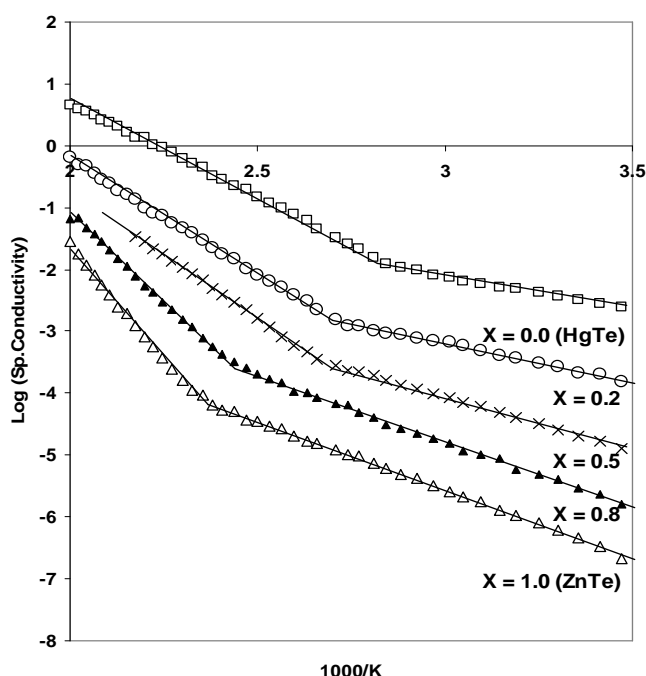
Figure 4: A plot of Log of conductivity versus reciprocal of temperature(in K) for samples with x = 0, 0.2, 0.5, 0.8 and 1.

_____

Table 1

Sr No	Composition	Thickness in micrometer	Cell size	Band gaps in eV	Activation energy (eV)	
					HT	**LT**
1.	ZnTe	0.80	6.033	2.33	0.505	0.188
2.	Zn0.9Hg0.1Te	0.87	6.090	2.14	0.473	0.173
3.	Zn0.8Hg0.2Te	0.90	6.122	1.93	0.471	0.156
4.	Zn0.7Hg0.3Te	0.98	6.183	1.75	0.327	0.140
5.	Zn0.6Hg0.4Te	1.11	6.216	1.54	0.282	0.125
6.	Zn0.5Hg0.5Te	1.13	6.252	1.31	0.215	0.115
7.	Zn0.4Hg0.6Te	1.16	6.284	1.12	0.197	0.110
8.	Zn0.3Hg07Te	1.23	6.330	0.93	0.163	0.097
9.	Zn0.2Hg0.8Te	1.28	6.363	0.72	0.151	0.086
10.	Zn0.1Hg0.9Te	1.30	6.411	0.50	0.121	0.075
11.	HgTe	1.34	6.462	0.31	0.106	0.066

The temperature dependence of electrical conductivity of a normal semiconductor shows two conduction behavior, one at higher temperature, that is governed by thermo ionic emissions over the grain boundaries (the intrinsic type of conductivity) while second at low temperature, due to thermally assisted hopping between nearest neighbors close to Fermi levels (called extrinsic conductivity). Accordingly we observed two linear portions in the plot of log σ Vs 1000/T for ZMT film. The slope of the lines exhibit a decrease in its magnitudes with increase in mercury content indicating degenerate nature of the deposits. A positive value of slope for HgTe indicates that HgTe is semiconducting in nature. The activation energies calculated from the slopes of the linear portions fall in the range 0.505 eV to 0.106 eV (For high temp. region) and 0.188 eV to 0.066 eV (for low temp. region). The dark specific conductance of HgTe film was found to be 1.28×10^4 $(\Omega cm)^{-1}$ while that of ZnTe film was found to be 2.8×10^6 $(\Omega cm)^{-1}$.

According to Rao [28], the nature of charge carriers (whether n or p type) in the ZMT films has been estimated from thermoelectric power measurements. The sign of terminal at the cold end used to measure thermo emf, was positive for films with $x \leq 0.5$ at cold indicating p type nature of films while films with $x \geq 0.5$ showed n-type behavior.

CONCLUSION

A ternary n-type ZnHgTe alloy material, in cubic, stoichiometric form can be deposited easily by this novel method. The results of XRD, Elemental and Optical Absorption analyses are in confirmatory of ZnHgTe alloy formation. The crystallinity, electrical conductivities were found to increase; while band gaps and conduction activation energies were found decreased with addition of Hg progressively without any anomalies. Ternary ZMT with $x \leq 0.5$ were p type while those with $x \geq 0.5$ showed n-type behavior.

_____

REFERENCES

[1] T Mahalingum, A.Kathalingam, S Velumani, S. Lee, H. Moon & Y.D. Kim, *J Nanomaterials for Electrochemical System*s, 10 (**2007**) 21-25.
[2] J. M. Gaines, R. R. Drenten, K. W. Haberern, T. Marshell, P. Mensz and J. Petruzzello, *Appl. Phys. Lett.* 62 (**1993**) 2462.
[3] A. Rogal'skiœ, *Infrared Detectors* (Nauka, Novosibirsk, **2003**) [in Russian].
[4] V.G. Deibuk, S.G. Dremlyuzhenko, S.E. Ostapov, *Semiconductors*, 39 (**2005**) 1111-1116.
[5] Ariel Sher, D. Eger, and A. Zemel, *Appl. Phys. Lett*. 46 (1) (**1985**) 59.
[6] J C Woolley and B Ray, *J. Phys. Chem. Solids* 13 (**1960**) 151-153.
[7] A. Sher, A.B. Chen, W.E Spicer, C.K. Shih, *J Vac. Sci. Technol*, A3 (**1985**) 105-111.
[8] A. Rogalski, *Infrared Phys*. 31 (**1991**) 117.
[9] A. Rogalski, *Prog. Quantum Electron*. 13 (**1989**) 299.
[10] E.M. Sheregii, *Optoelectronic Review*, 3-4 (**1995**) 95-98.
[11] V.N. Sochinski, J.C. Soares, E. Alves, *Semicond. Sci. Technol*, 11 (**1996**) 542.
[12] S. Sivanatha, X. Chu, M. Boukerch, and J. P. Faurie, *Appl. Phi. Lctt*, 47 (**1985**) 1291.
[13] K.T. Chert, Y. G. Sha, and R. F. Brebrick, *J. Vac. Sci. Technol*. **1086** (1990).
[14] C. Thero, P.Singh, Photovoltaic Specialists Conference, **1996**, Conference Record of the Twenty Fifth IEEE, page(s): 941 - 943 Meeting Date: 13 - 17 May 1996, Washington, DC , USA Print ISBN: 0-7803-3166-4
[15] Ariel Sher. and Alex Tsigelman, *J. Vac. Sci. Technol*.A-8 (**1990**) 1093.
[16] R.Granger. and C.M. Pelletier, *J. Cryst. Growth*.117, (**1992**) 203.
[17] S. Rolland, R. Granger and R. Triboulet, *J. Cryst. Growth,* 117 (**1992**) 208.
[18] P. P. Hankare, V. M. Bhuse, K. M. Garadkar, S. D. Delekar and P. R. Bhagat, *Semicond. Sci. Technol.,* **2004**, 19, 277.
[19] P.P. Hankare, P.A. Chate, S.D. Delekar, V.M. Bhuse, M.R. Asabe, B.V. Jadhav, K.M. Garardkar, *J. Cryst. Growth*., **2006**, 291, 40.
[20] P. P. Hankare, S. D. Delekar, P. A. Chate, S. D. Sabane, K. M. Garadkar and V. M. Bhuse, *Semicond. Sci. Technol*., **2005**, 20, 257.
[21] U.R. Dappadwad, M.K. Lande, S.G. Chonde, B.R. Arbad, P.P. Hankare, V.M. Bhuse, *Mater*. *Chem. Phys.,* **2008**, 112, 941.
[22] B.R. Arbad, S.G. Chonde, P.P. Hankare, V.M. Bhuse, *Achieves of Applied Science Research*, 3(2) (**2011**) 422.
[23] T. Ohgai, T. Ikeda, Y. Kawanaka, K. Takao, A. Kagawa, *Material Science Forum*, 654-656 (**2010**) 1732-1735.
[24] Vogel's Text Book of Quantitative Chemical Analysis, Fifth Edition, (Editors) G.H Jeffery, J. Bassett, J. Mendham, R.C. Denney, Longman Scientific & Technical, UK **1989**, pp-46
[25] M. A. M. Seyam, A. Elfalaky, *Vacuum*, **2000**, 57, 31.
[26] M.C. Petty and C. Juhasz *J. Phys. D: Appl. Phys*., 9 (**1976**) 1605-17.
[27] R. L. Pertritz, *Phys. Rev*., **1965**, 104, 1508.
[28] C. N. R. Rao, Modern Aspects of Solid State Chemistry, Plenum Press, New York, **1970**. p-141.